PERGAMON

Annals of Nuclear Energy 27 (2000) 1627–1642

annals of
NUCLEAR ENERGY

www.elsevier.com/locate/anucene

Gamma displacement cross-sections in various materials

Junhyun Kwon, Arthur T. Motta *

Department of Mechanical and Nuclear Engineering, The Pennsylvania State University, University Park, PA 16802, USA

Received 17 January 2000; accepted 15 February 2000

Abstract

The gamma displacement cross-sections for energies up to 14 MeV have been calculated in various materials at two values of displacement threshold energy (24 and 40 eV). Three types of gamma ray interactions with materials are considered, the photoelectric effect, Compton scattering and pair production. Depending on the atomic number (Z) of target materials and energy of incident gamma rays, the relative contribution of three interactions to total displacements changes. It is found that for medium and low-Z material Compton scattering is predominant over most of the energy range, while pair production becomes important for high-Z material at high gamma energy.

1. Introduction

There has been some recent interest in gamma ray damage in metals prompted by its role in promoting accelerated embrittlement of reactor pressure vessel (RPV) steels in the HFIR reactor (Rehn and Birtcher, 1993; Farrell et al. 1994). Whereas the impact of fast neutrons ($E_n > 1$MeV) on material property changes is clearly recognized, the impact of gamma ray damage to materials is usually not significant. However in situations where there is a large water gap, gamma damage can become comparable to that produced by neutrons, on a straight displacements per atom (dpa) basis. A recent analysis of gamma ray displacement damage in the RPV of the General Electric (GE) Advanced Boiling Water Reactor (ABWR) indicated that the calculated gamma displacement damage is higher than the neutron-induced

* Corresponding author. Tel.: +1-814-865-0036; fax: +1-814-865-8499.
E-mail address: atm2@psu.edu (A.T. Motta).

0306-4549/00/$ - see front matter
PII: S0306-4549(00)00024-4

displacement damage rates at the RPV inner diameter (Alexander and Rehn, 1994). Also, because gamma rays are much more efficient than neutrons at producing freely-migrating defects (Rehn and Birtcher, 1993), any radiation-enhanced or radiation-induced processes that depend on the magnitude of long-range defect fluxes to sinks (such as radiation induced segregation, irradiation creep, void swelling, etc.), can be disproportionately affected by gamma damage. In those cases, the effect of point defects produced by gamma ray damage on mass transport kinetics could be dominant over those produced by fast neutrons.

The direct evaluation of the contribution of gamma ray to damage in materials in dpa, is possible once the gamma displacement damage cross sections are known. While the calculation of neutron-induced displacement damage can be performed using the SPECTER computer code (Greenwood and Smither, 1985), the lack of experimental and analytical data on gamma displacement cross sections hinders the quantification of such damage. Evaluations of gamma displacements in iron have been published previously. Alexander (Alexander, 1997) performed a calculation of the gamma displacement cross section in iron, using the McKinley–Fesbach approximation for the electron displacement cross sections. Using analytical expressions for the gamma–electron interaction (Compton scatter and pair production) and using Oen's electron displacement cross-sections (Oen, 1973), Baumann calculated the gamma displacement cross sections for iron (Baumann, 1990). In this article we use a similar approach to calculate cross sections in various materials in the energy range from 0 to 14 MeV. The three types of gamma ray interactions with materials are taken into account, i.e. Compton scattering, photoelectric effect, and pair production. For comparative purposes, two values of the displacement threshold energy (24 and 40 eV) are used. Additional consideration is given to the possible displacement cascade effects in iron resulting from high-energy electrons.

2. Methodology

Gamma rays can displace atoms by first transferring energy to an electron, which transfers energy to a lattice atom through an electron-atom scattering event. The energetic electrons can be produced from Compton scattering, photoelectric effect and pair production. Therefore, the total gamma displacement cross-section consists of three components representing the sum of cross-sections for three interactions,

$$\sigma_\gamma^{\mathrm{T}}(E_\gamma) = \sigma_\gamma^{\mathrm{PE}}(E_\gamma) + \sigma_\gamma^{\mathrm{CS}}(E_\gamma) + \sigma_\gamma^{\mathrm{PP}}(E_\gamma) \tag{1}$$

where E_γ is the gamma incident energy and the superscripts PE, CS, and PP represent photoelectric effect, Compton scattering, and pair production, respectively.

2.1. Photoelectric effect displacement cross-section (σ_γ^{PE})

For gamma ray energies below 0.1 MeV, the dominant mode of interaction of the gamma ray with material is the photoelectric effect. In this process, a gamma ray is

absorbed by an atom and then an energetic photoelectron is ejected from one of its bound shells. The ejected electron possesses kinetic energy E_0, which is equal to the incident gamma energy E_γ minus the binding energy (BE) of the electron to the atom. Under the assumption that all electrons have the same initial energy for the given gamma energy of E_γ resulting from K-shell ionization, the photoelectric effect displacement cross-section is given by

$$\sigma_\gamma^{\mathrm{PE}}(E_\gamma) = \sigma^{\mathrm{PE}}(E_\gamma, E_0)\cdot\bar{n}(E_0) \tag{2}$$

where $\bar{n}(E_0)$ is the total number of displaced atoms produced on the average over the range of the recoil electron of energy E_0.

The analytical equations of the photoelectric effect cross-section, $\sigma_\gamma^{\mathrm{PE}}(E_\gamma, E_0)$ in Eq. (2), can be obtained for the three energy regions: (a) $E_\gamma < 0.35\,\mathrm{MeV}$, (b) $0.35\,\mathrm{MeV} < E_\gamma < 2\,\mathrm{MeV}$, and (c) $E_\gamma > 2$ MeV. In region (a), we can use Sauter's equation (Davisson and Evans, 1952):

$$\sigma^{\mathrm{PE}}(E_\gamma, E_0) = \frac{3}{2}\varphi_{\mathrm{o}}\frac{Z^5}{137^4}\xi^5(\Lambda^2-1)^{3/2} \times\left[\frac{4}{3}+\frac{\Lambda(\Lambda-2)}{\Lambda+1}\left(1-\frac{1}{2\Lambda(\Lambda^2-1)^{1/2}}\cdot\ln\frac{\Lambda+(\Lambda^2-1)^{1/2}}{\Lambda-(\Lambda^2-1)^{1/2}}\right)\right] \tag{3}$$

where Z is the atomic number of the material and Λ is given by

$$\Lambda = \frac{E_\gamma - BE - E_{\mathrm{e}}}{E_{\mathrm{e}}} \tag{4}$$

The parameter ξ in Eq. (3) is the ratio of electron rest mass energy E_{e} to incident gamma energy E_γ, and φ_{o} is the Thompson cross-section, 0.6653 barn.

In the energy region (b), no simple cross-section formula is available. Because of this, Sauter's equation, which is applicable to case (a), was used for the calculation. The results from this approximation should be accurate within 4% as compared to numerical solutions for region (b). In region (c) we employ Hall's equation given by (Davisson and Evans, 1952),

$$\begin{aligned}\sigma^{\mathrm{PE}}(E_\gamma, E_0) = {} & \frac{5}{4}\frac{Z^5}{137^4}\frac{1}{E_\gamma}\exp\left\{-\frac{\pi Z}{137}+2\left(\frac{Z}{137}\right)^2\left(1-\ln\frac{Z}{137}\right)\right\} \\ & \times\left\{\frac{(E_0^2+2E_0)^{3/2}}{E_\gamma^2}\right\}\left\{\frac{4}{3}+\frac{E_0^2-1}{E_0+2}\right. \\ & \left.\times\left[1-\frac{1}{2(E_0+1)(E_0^2+2E_0)^{1/2}}\cdot\ln\left(\frac{E_0+1+(2E_0+E_0^2)^{1/2}}{E_0+1-(2E_0+E_0^2)^{1/2}}\right)\right]\right\} \\ & \times 10^{-24}\ \mathrm{cm}^2\end{aligned} \tag{5}$$

The $\bar{n}(E_0)$ in Eq. (2) is calculated by integrating over the initial electron kinetic energy E_0

$$\bar{n}(E_0) = N_a \int_0^{E_0} \frac{\sigma_d^e(E)}{(-dE/dx)} dE \tag{6}$$

where N_a is the atomic number density of the material, $(-dE/dx)$ is the electronic stopping power, and $\sigma_d^e(E)$ is the electron displacement cross-section. The electronic stopping power (in units of eV/cm) of the material represents the change in electron energy with distance as the electron traverses the material, and is given by

$$-\frac{dE}{dx} = \frac{2\pi e^4 N_a Z(3\times 10^9)^4}{E_e \beta^2 (1.6\times 10^{-6})^2} \left\{ \ln\left[\frac{E_e E \beta^2}{I_p^2(1-\beta^2)}\right] - \beta^2 \right\} \tag{7}$$

where I_p is the mean ionization potential of sample atoms ($=1.35\times10^{-5}$ Z MeV) (Cember, 1983), β represents the ratio of the velocity of the electron to the velocity of light and e is the electron charge ($=1.602\times10^{-19}$ Coulomb).

We solved Eq. (5) numerically using the results of the electron displacement cross-section, $\sigma_d^e(E)$ developed by Oen (1973) on the basis of the McKinley–Fesbach formula. In the report (Oen, 1973), $\sigma_d^e(E)$ is tabulated as a function of displacement threshold energy and elements. Since the variation of cross-section with the electron energy is well-behaved, we applied a piece-wise interpolation of $\sigma_d^e(E)$ to obtain $\bar{n}(E_0)$. Using the calculation results of $\bar{n}(E_0)$ derived above, the photoelectric effect displacement cross section can be obtained by combining Eqs. (3)–(7).

2.2. Compton scattering displacement cross-section (σ_γ^{CS})

Compton scattering takes place between the incident gamma ray and orbital electrons in material. This interaction is the predominant mechanism at intermediate gamma ray energies, ranging from 0.1 to 10 MeV in metals. In Compton scattering, the incoming gamma ray is deflected by a certain angle with respect to its incident direction, and thus imparts a portion of its energy to the electron at rest, which then becomes the recoil electron.

The desired displacement cross section for Compton scattering is (Oen and Holmes, 1959),

$$\sigma_\gamma^{CS}(E_\gamma) = \int_0^{E_0^{max}} \frac{d\sigma^c(E_\gamma, E_0)}{dE_0} \cdot \bar{n}(E_0) dE_0 \tag{8}$$

where the kinetic energy of the recoil electron E_0 is a function of scattering angle θ; $d\sigma^c(E_\gamma, E_0)/dE_0$ is the differential scattering cross-section, given by the Klein–Nishina formula. The relationship between the energy of the incident gamma ray and that of the recoil electron is expressed in terms of scattering angle θ as

$$E_0 = \frac{E_\gamma(1-\cos\theta)}{(E_e/E_\gamma) + (1-\cos\theta)} \tag{9}$$

where E_e is the electron rest mass energy ($=0.511$ MeV). When $\theta = \pi$ in Eq. (9), the electron has the maximum energy, which corresponds to E_0^{max} in Eq. (8). The Klein–Nishina formula for determining the scattering cross-section for gamma ray interaction with electrons is

$$\frac{d\sigma^c(E_\gamma, E_0)}{dE_0} = \frac{\pi e^4 Z}{E_e(E_\gamma - E_0)^2} \cdot \left\{ \left[\frac{E_e E_0}{E_\gamma^2}\right]^2 + 2\left[\frac{E_\gamma - E_0}{E_\gamma}\right]^2 + \frac{E_\gamma - E_0}{E_\gamma^3}\left[(E_0 - E_e)^2 - E_e^2\right] \right\} \quad (10)$$

Combining the calculation results of $\bar{n}(E_0)$ and Eq. (10), the Compton scattering displacement cross-section can be calculated.

2.3. Pair production displacement cross-section (σ_γ^{PP})

In the process of pair production, the gamma ray is completely absorbed in the field of the nucleus, and an electron–positron pair is created. Pair production is energetically possible only if the gamma ray energy exceeds 1.02 MeV, which corresponds to twice the rest mass energy of an electron. Any excess energy carried by the gamma ray is assumed to be completely converted to kinetic energy shared by the positron and electron. Because the positron subsequently annihilates by combining with an electron, its effect on atomic displacement is not included in the calculation. Similarly to the photoelectric effect, the pair production displacement cross-section is given by (Evans, 1955)

$$\sigma_\gamma^{PP}(E_\gamma) = \sigma^{PP}(E_\gamma, E_0) \cdot \bar{n}(E_0) \quad (11)$$

where

$$\sigma^{PP}(E_\gamma, E_0) = \sigma_{co} \cdot Z^2 \left\{ \frac{28}{9} \ln\left(\frac{2E_\gamma}{E_e}\right) - \frac{218}{27} \right\} \quad (12)$$

The value of σ_{co} in Eq. (12) is 2.8×10^{-4} barn.

3. Results

The gamma ray displacement cross sections calculated for the three processes are presented for nine different elements: C, Si, Cr, Fe, Ni, Mo, Ag, Au and U, representing a broad range of atomic numbers. In these calculations, two displacement threshold energies (E_d) of 24 and 40 eV were used. The photoelectric effect displacement cross-sections are provided in Fig. 1(a) and (b) for two different threshold energies. Figs. 2 and 3 show the calculated Compton scattering and pair production

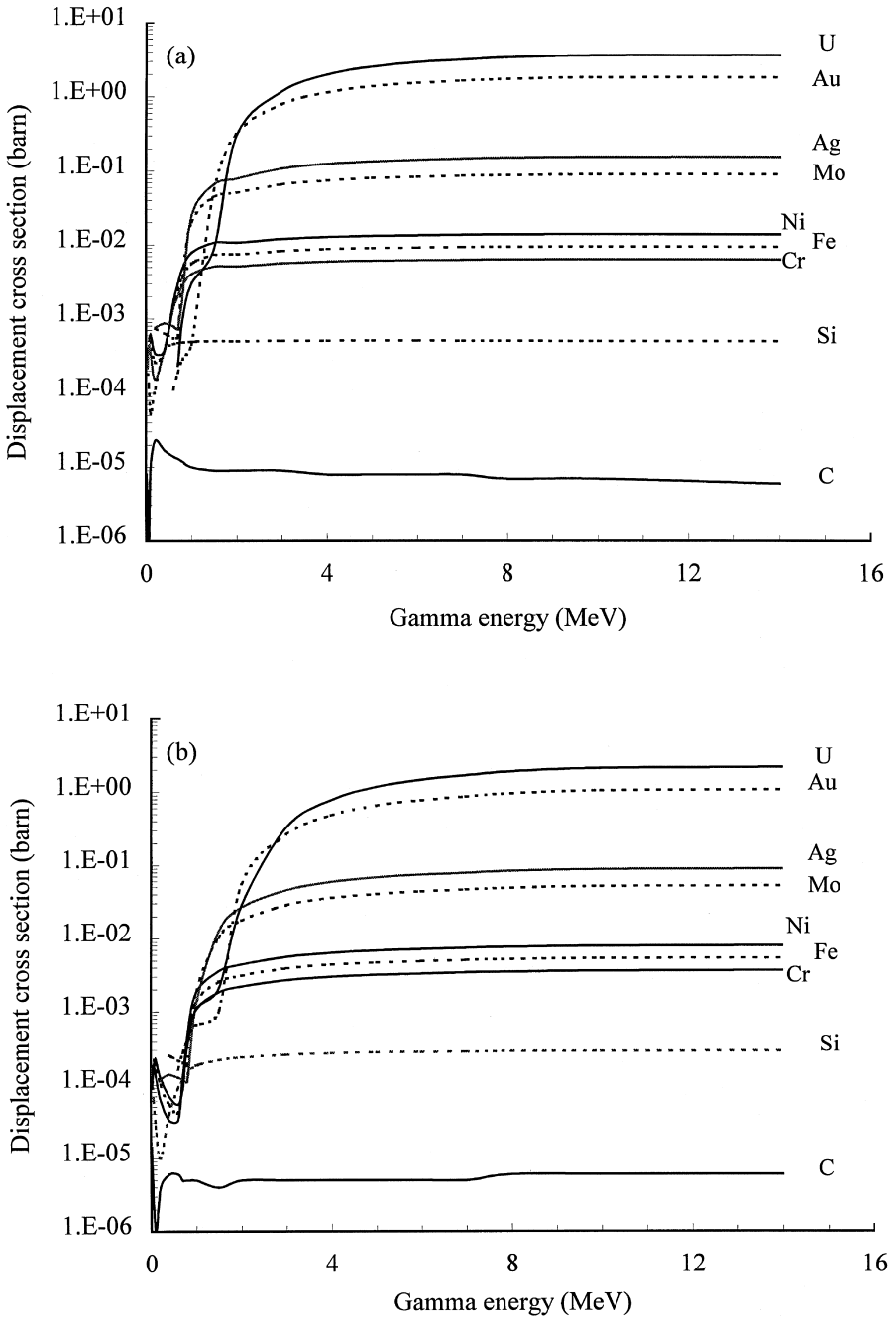

Fig. 1. Displacement cross-sections as a function of gamma energy, in various materials for the photoelectric effect at the displacement threshold energy of 24 eV (a) and 40 eV(b).

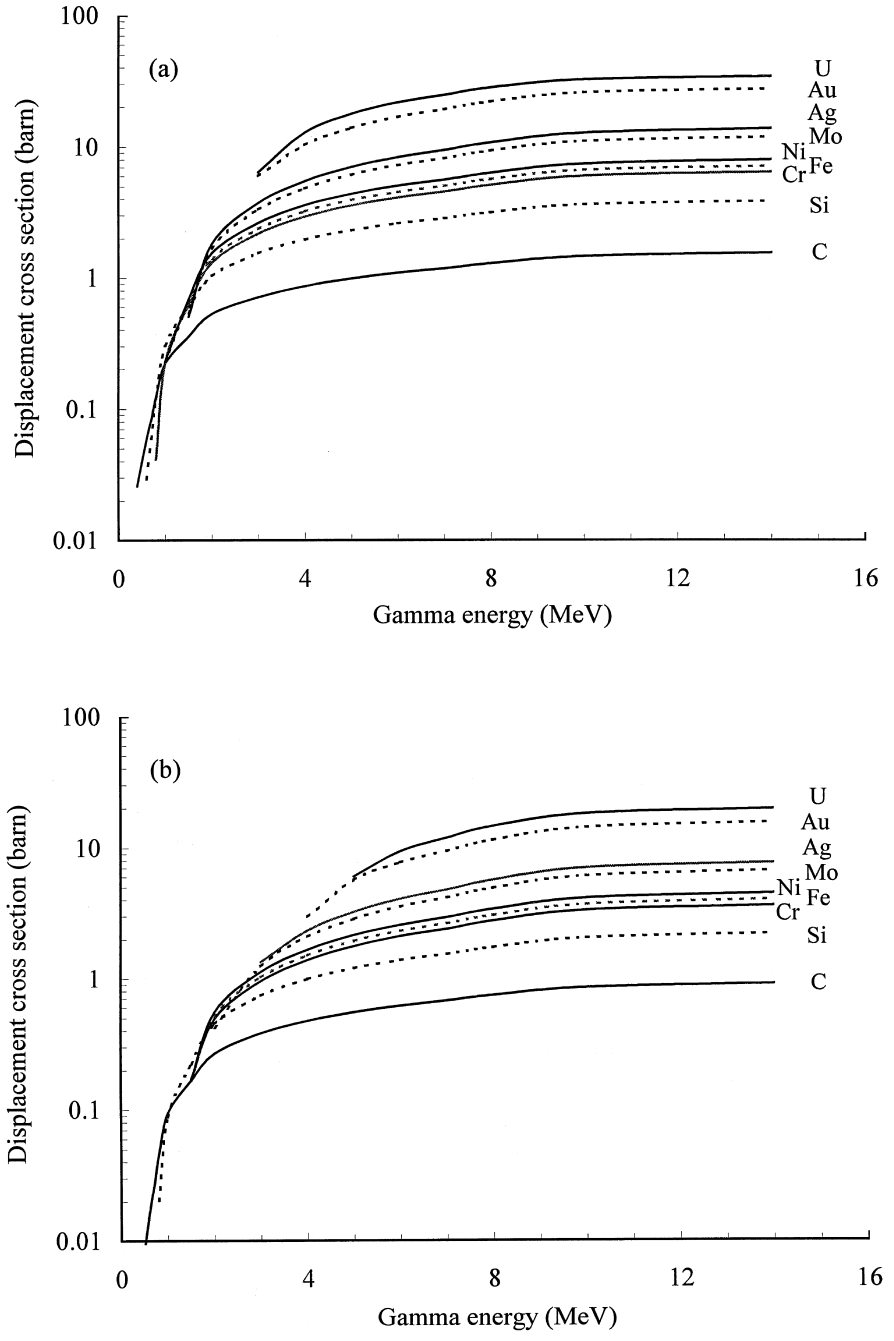

Fig. 2. Displacement cross-sections in various materials for the Compton scattering at the displacement threshold energy of 24 eV (a) and 40 eV (b).

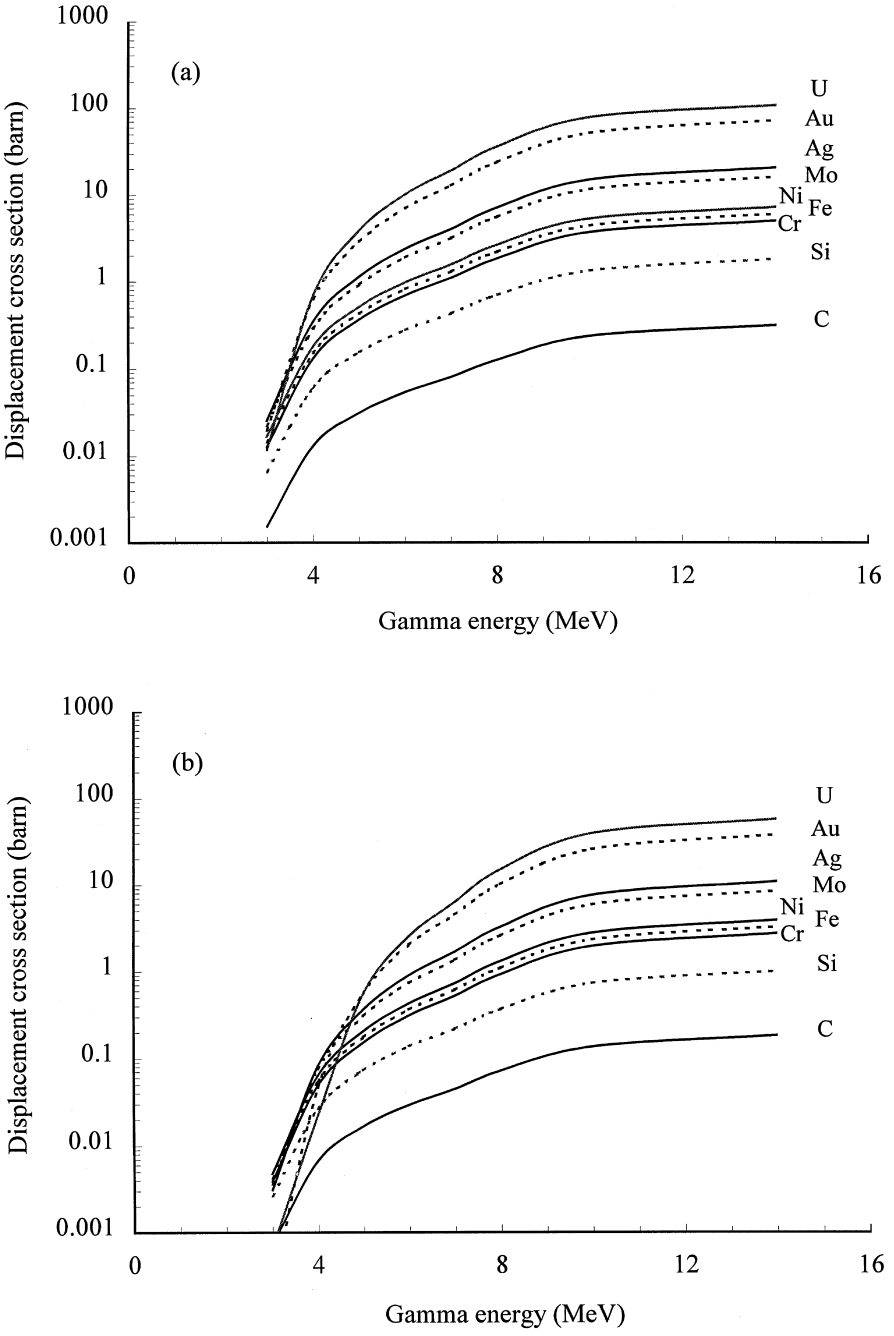

Fig. 3. Displacement cross-sections in various materials from pair production at the displacement threshold energy of 24 eV (a) and 40 eV (b).

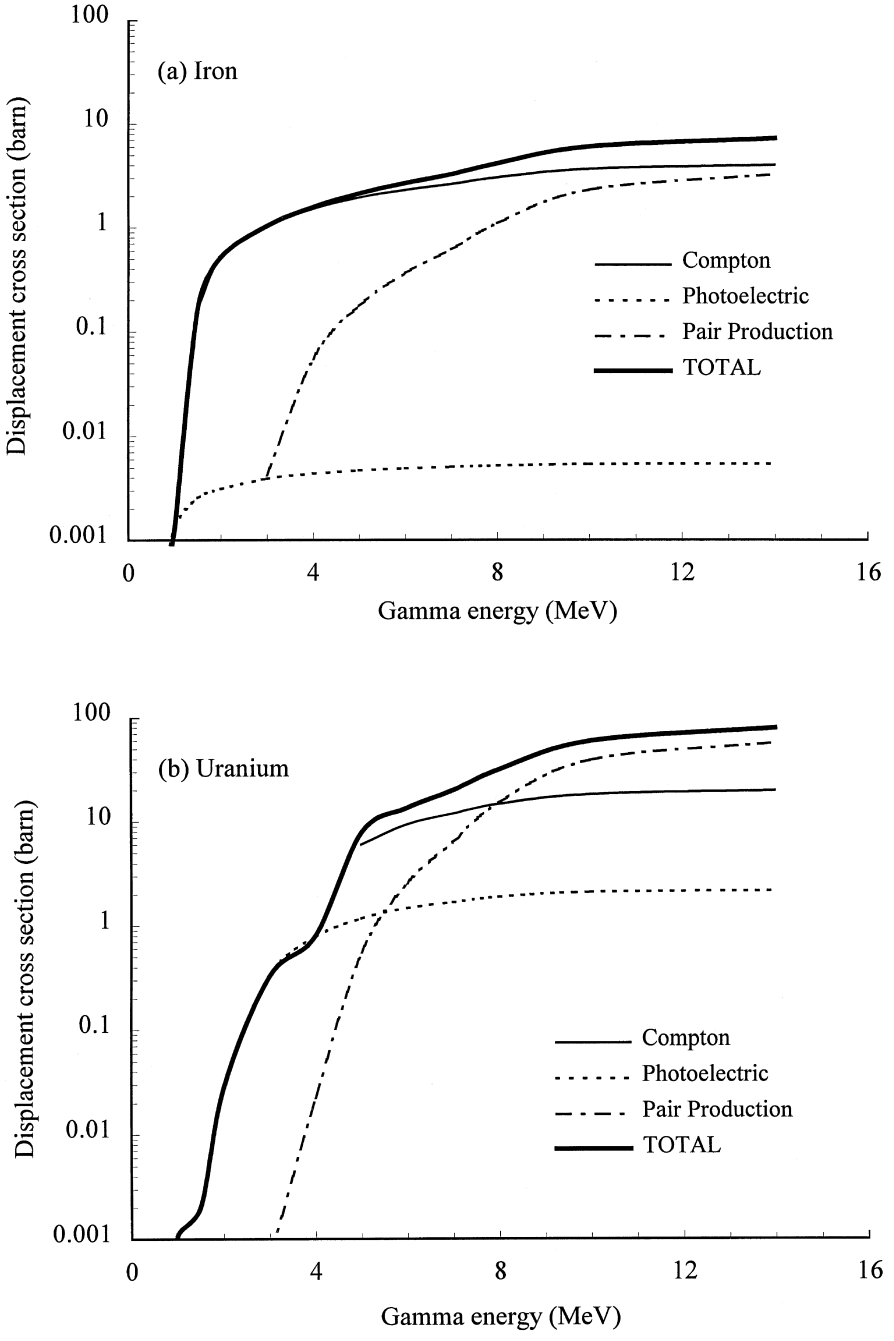

Fig. 4. Total displacement cross sections for gamma ray interactions in (a) iron and (b) uranium at $E_d = 40$ eV.

Table 1
Displacement cross-sections for gamma ray interactions with various materials (unit: barn)

	$E_d = 24$ eV			$E_d = 40$ eV		
Gamma energy (MeV)	Compton scattering	Photoelectric effect	Pair production	Compton scattering	Photoelectric effect	Pair production
Carbon						
0.2	0.00	2.3E-05	0.00	0.00	4.0E-06	0.00
0.4	0.03	1.7E-05	0.00	0.00	6.0E-06	0.00
0.6	0.06	1.4E-05	0.00	0.02	6.0E-06	0.00
0.7	0.08	1.3E-05	0.00	0.03	5.0E-06	0.00
0.8	0.12	1.2E-05	0.00	0.04	5.0E-06	0.00
1	0.22	1.0E-05	0.00	0.09	5.0E-06	0.00
1.5	0.36	9.0E-06	0.00	0.17	4.0E-06	0.00
2	0.53	9.0E-06	0.00	0.27	5.0E-06	0.00
3	0.72	9.0E-06	0.00	0.38	5.0E-06	0.00
4	0.87	8.0E-06	0.01	0.48	5.0E-06	0.01
5	0.99	8.0E-06	0.03	0.56	5.0E-06	0.02
6	1.10	8.0E-06	0.05	0.62	5.0E-06	0.03
7	1.19	8.0E-06	0.08	0.68	5.0E-06	0.05
8	1.30	7.0E-06	0.13	0.75	6.0E-06	0.07
10	1.47	7.0E-06	0.24	0.86	6.0E-06	0.14
14	1.57	6.0E-06	0.32	0.92	6.0E-06	0.19
Silicon						
0.2	0.00	1.2E-04	0.00	0.00	1.0E-05	0.00
0.4	0.00	3.9E-04	0.00	0.00	3.9E-05	0.00
0.6	0.03	4.6E-04	0.00	0.00	9.1E-05	0.00
0.7	0.06	4.7E-04	0.00	0.00	1.2E-04	0.00
0.8	0.12	4.8E-04	0.00	0.02	1.4E-04	0.00
1	0.30	4.9E-04	0.00	0.09	1.8E-04	0.00
1.5	0.60	5.0E-04	0.00	0.22	2.2E-04	0.00
2	1.04	5.0E-04	0.00	0.45	2.4E-04	0.00
3	1.55	5.1E-04	0.01	0.74	2.6E-04	0.00
4	1.97	5.1E-04	0.06	1.00	2.7E-04	0.03
5	2.31	5.1E-04	0.16	1.21	2.8E-04	0.07
6	2.61	5.1E-04	0.28	1.39	2.8E-04	0.14
7	2.86	5.1E-04	0.43	1.55	2.8E-04	0.22
8	3.17	5.1E-04	0.70	1.75	2.9E-04	0.37
10	3.65	5.0E-04	1.35	2.06	2.9E-04	0.74
14	3.91	5.0E-04	1.83	2.23	2.9E-04	1.01
Chromium						
0.2	0.00	1.5E-04	0.00	0.00	6.4E-05	0.00
0.4	0.00	3.9E-04	0.00	0.00	3.3E-05	0.00
0.6	0.00	1.4E-03	0.00	0.00	3.3E-05	0.00
0.7	0.00	2.0E-03	0.00	0.00	1.2E-04	0.00
0.8	0.04	2.8E-03	0.00	0.00	3.9E-04	0.00
1	0.23	4.1E-03	0.00	0.00	1.1E-03	0.00
1.5	0.62	5.1E-03	0.00	0.17	1.8E-03	0.00
2	1.31	5.1E-03	0.00	0.49	2.2E-03	0.00

(Table continued on next page)

Table 1 (*continued*)

	$E_d = 24$ eV			$E_d = 40$ eV		
Gamma energy (MeV)	Compton scattering	Photoelectric effect	Pair production	Compton scattering	Photoelectric effect	Pair production
3	2.19	5.7E-03	0.01	0.96	2.7E-03	0.00
4	2.94	5.9E-03	0.13	1.40	3.0E-03	0.05
5	3.58	6.1E-03	0.37	1.79	3.2E-03	0.15
6	4.12	6.2E-03	0.70	2.12	3.3E-03	0.31
7	4.58	6.3E-03	1.12	2.42	3.4E-03	0.53
8	5.16	6.3E-03	1.87	2.79	3.5E-03	0.93
10	6.05	6.4E-03	3.73	3.36	3.6E-03	1.96
14	6.53	6.4E-03	5.12	3.66	3.6E-03	2.75
Iron						
0.2	0.00	2.6E-04	0.00	0.00	1.0E-04	0.00
0.4	0.00	3.7E-04	0.00	0.00	5.4E-05	0.00
0.6	0.00	1.5E-03	0.00	0.00	4.2E-05	0.00
0.7	0.00	2.4E-03	0.00	0.00	1.0E-04	0.00
0.8	0.00	3.7E-03	0.00	0.00	4.2E-04	0.00
1	0.22	5.6E-03	0.00	0.00	1.4E-03	0.00
1.5	0.65	7.4E-03	0.00	0.17	2.6E-03	0.00
2	1.40	7.4E-03	0.00	0.52	3.1E-03	0.00
3	2.38	8.3E-03	0.01	1.03	3.9E-03	0.00
4	3.22	8.8E-03	0.15	1.52	4.4E-03	0.06
5	3.93	9.0E-03	0.43	1.95	4.7E-03	0.18
6	4.54	9.2E-03	0.83	2.33	4.9E-03	0.37
7	5.06	9.3E-03	1.32	2.65	5.1E-03	0.62
8	5.70	9.4E-03	2.23	3.07	5.2E-03	1.10
10	6.70	9.5E-03	4.46	3.71	5.4E-03	2.33
14	7.24	9.5E-03	6.12	4.06	5.4E-03	3.28
Nickel						
0.2	0.00	3.4E-04	0.00	0.00	1.3E-04	0.00
0.4	0.00	3.7E-04	0.00	0.00	7.1E-05	0.00
0.6	0.00	1.7E-03	0.00	0.00	5.4E-05	0.00
0.7	0.00	3.0E-03	0.00	0.00	9.0E-05	0.00
0.8	0.00	4.8E-03	0.00	0.00	4.7E-04	0.00
1	0.23	7.8E-03	0.00	0.00	1.8E-03	0.00
1.5	0.69	1.1E-02	0.00	0.17	3.6E-03	0.00
2	1.55	1.1E-02	0.00	0.56	4.4E-03	0.00
3	2.64	1.2E-02	0.02	1.13	5.7E-03	0.00
4	3.59	1.3E-02	0.18	1.68	6.4E-03	0.06
5	4.40	1.3E-02	0.52	2.17	6.9E-03	0.21
6	5.08	1.4E-02	0.99	2.59	7.2E-03	0.43
7	5.66	1.4E-02	1.59	2.96	7.4E-03	0.73
8	6.39	1.4E-02	2.68	3.43	7.7E-03	1.31
10	7.50	1.4E-02	5.38	4.15	7.9E-03	2.81
14	8.10	1.4E-02	7.39	4.54	8.0E-03	3.94

(Table continued on next page)

Table 1 (*continued*)

	$E_d = 24$ eV			$E_d = 40$ eV		
Gamma energy (MeV)	Compton scattering	Photoelectric effect	Pair production	Compton scattering	Photoelectric effect	Pair production
Molybdenum						
0.2	0.00	7.5E-04	0.00	0.00	3.0E-04	0.00
0.4	0.00	6.4E-04	0.00	0.00	2.6E-04	0.00
0.6	0.00	5.5E-04	0.00	0.00	2.2E-04	0.00
0.7	0.00	5.7E-04	0.00	0.00	2.0E-04	0.00
0.8	0.00	3.6E-03	0.00	0.00	1.8E-04	0.00
1	0.00	2.0E-02	0.00	0.00	1.9E-03	0.00
1.5	0.54	4.5E-02	0.00	0.00	1.0E-02	0.00
2	1.68	5.1E-02	0.00	0.43	1.8E-02	0.00
3	3.33	6.6E-02	0.02	1.25	2.9E-02	0.00
4	4.84	7.5E-02	0.29	2.10	3.6E-02	0.08
5	6.15	8.1E-02	0.93	2.88	4.0E-02	0.31
6	7.26	8.4E-02	1.91	3.57	4.4E-02	0.74
7	8.21	8.7E-02	3.20	4.17	4.6E-02	1.35
8	9.39	8.9E-02	5.62	4.93	4.9E-02	2.59
10	11.16	9.1E-02	11.73	6.11	5.1E-02	5.91
14	12.10	9.2E-02	16.31	6.74	5.2E-02	8.48
Silver						
0.2	0.00	7.6E-04	0.00	0.00	1.2E-04	0.00
0.4	0.00	8.7E-04	0.00	0.00	1.4E-04	0.00
0.6	0.00	7.9E-04	0.00	0.00	1.3E-04	0.00
0.7	0.00	7.5E-04	0.00	0.00	1.2E-04	0.00
0.8	0.00	1.9E-03	0.00	0.00	1.1E-04	0.00
1	0.00	2.5E-02	0.00	0.00	1.3E-03	0.00
1.5	0.51	6.6E-02	0.00	0.00	1.3E-02	0.00
2	1.82	8.0E-02	0.00	0.00	2.6E-02	0.00
3	3.74	1.1E-01	0.03	1.35	4.6E-02	0.00
4	5.52	1.3E-01	0.35	2.35	5.9E-02	0.08
5	7.05	1.4E-01	1.15	3.26	6.8E-02	0.37
6	8.36	1.4E-01	2.41	4.08	7.4E-02	0.90
7	9.48	1.5E-01	4.07	4.79	7.9E-02	1.68
8	10.85	1.5E-01	7.21	5.69	8.3E-02	3.28
10	12.90	1.6E-01	15.15	7.05	8.8E-02	7.59
14	14.02	1.6E-01	21.11	7.77	9.0E-02	10.94
Gold						
0.2	0.00	0.0E+00	0.00	0.00	0.0E+00	0.00
0.4	0.00	0.0E+00	0.00	0.00	0.0E+00	0.00
0.6	0.00	1.1E-04	0.00	0.00	1.6E-04	0.00
0.7	0.00	1.9E-04	0.00	0.00	2.8E-04	0.00
0.8	0.00	2.9E-04	0.00	0.00	4.2E-04	0.00
1	0.00	4.5E-04	0.00	0.00	6.7E-04	0.00
1.5	0.00	5.5E-02	0.00	0.00	9.7E-04	0.00
2	0.00	3.3E-01	0.00	0.00	5.5E-02	0.00
3	6.05	7.9E-01	0.02	0.00	2.6E-01	0.00

(Table continued on next page)

Table 1 (*continued*)

	$E_d = 24$ eV			$E_d = 40$ eV		
Gamma energy (MeV)	Compton scattering	Photoelectric effect	Pair production	Compton scattering	Photoelectric effect	Pair production
4	10.36	1.1E+00	0.63	3.00	4.8E-01	0.05
5	13.98	1.4E+00	2.90	5.68	6.5E-01	0.57
6	16.94	1.5E+00	7.07	7.76	7.7E-01	2.04
7	19.37	1.6E+00	12.92	9.48	8.6E-01	4.56
8	22.19	1.7E+00	24.21	11.52	9.5E-01	10.14
10	26.06	1.8E+00	52.57	14.39	1.0E+00	25.74
14	27.95	1.9E+00	73.52	15.82	1.1E+00	37.83
Uranium						
0.2	0.00	0.0E+00	0.00	0.00	0.0E+00	0.00
0.4	0.00	0.0E+00	0.00	0.00	0.0E+00	0.00
0.6	0.00	0.0E+00	0.00	0.00	0.0E+00	0.00
0.7	0.00	2.4E-04	0.00	0.00	8.5E-05	0.00
0.8	0.00	9.7E-04	0.00	0.00	3.5E-04	0.00
1	0.00	3.0E-03	0.00	0.00	1.1E-03	0.00
1.5	0.00	8.9E-03	0.00	0.00	2.1E-03	0.00
2	0.00	3.1E-01	0.00	0.00	2.8E-02	0.00
3	6.45	1.2E+00	0.01	0.00	3.3E-01	0.00
4	12.91	2.0E+00	0.70	0.00	7.8E−01	0.02
5	17.89	2.5E+00	3.91	6.04	1.2E+00	0.55
6	21.81	2.9E+00	10.25	9.42	1.5E+00	2.56
7	24.91	3.2E+00	19.29	11.91	1.7E+00	6.33
8	28.38	3.4E+00	36.73	14.67	1.9E+00	14.97
10	32.86	3.6E+00	79.63	18.28	2.1E+00	39.09
14	34.95	3.7E+00	100.74	19.97	2.2E+00	57.53

displacement cross-sections, respectively. Fig. 4 shows the relative contribution of the three gamma ray interaction processes to total displacement for iron and uranium at $E_d = 40$ eV. In addition, the numerical values of the gamma displacement cross sections in various materials are tabulated in Table 1, and the total displacement cross sections are plotted in Fig. 5. These calculation results are based on the assumption that the ejected electrons from three gamma ray interactions cause a single displacement. However, high energy electrons generated by high energy gamma can give enough energy to displaced atoms to induce secondary displacement reactions in sequence. Fig. 6 shows the effect of considering the "cascade" effect in calculating the iron displacement cross section, by using the values published by Oen (1973).

4. Discussion

The discontinuity of the photoelectric effect displacement cross-sections at gamma energy (less than 2 MeV) shown in Fig. 1 is due to the approximation involved in the use of Sauter's equation. The displacement cross sections for Fe with $E_d = 40$ eV

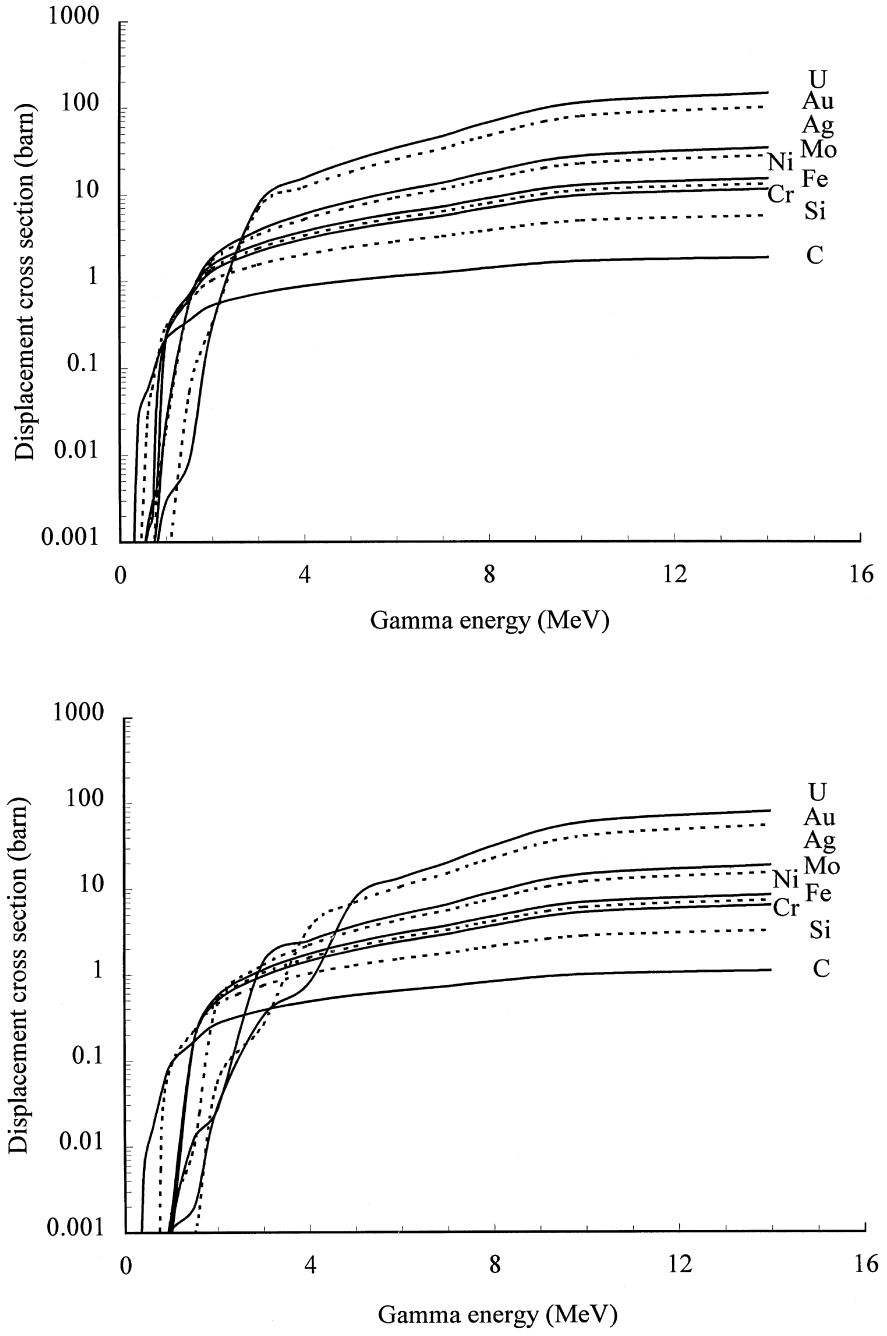

Fig. 5. Total displacement cross-sections for gamma ray interactions with materials at the displacement threshold energy of 24 eV (a) and 40 eV (b).

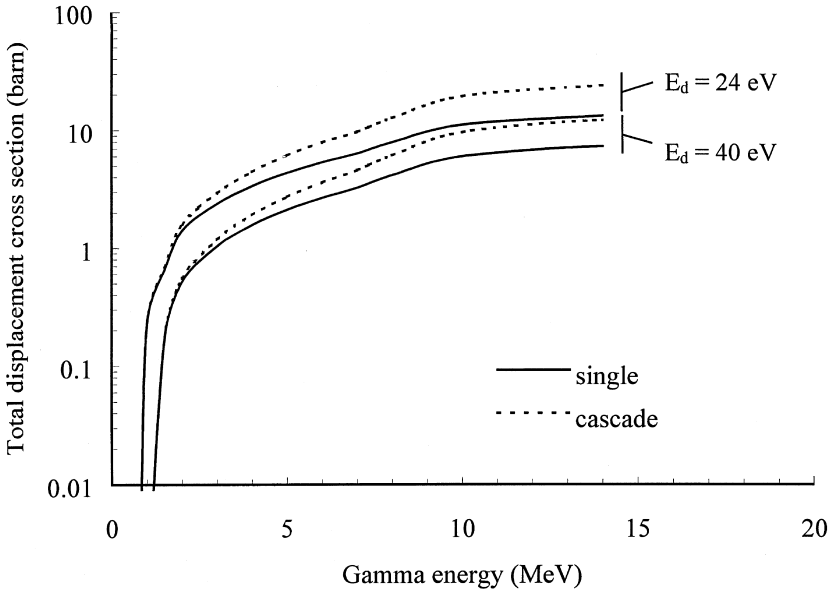

Fig. 6. Total displacement cross sections for gamma ray in iron as a function of gamma energy for two values of E_d, for the cases of single displacement (solid line) or cascade displacements (dotted line).

calculated in this work agree reasonably well with the previous calculations of Baumann and Alexander. We find that the total displacement cross section calculated in this work is within 5% of that calculated by Baumann (Baumann, 1990). We can attribute these differences to the different interpolation schemed we used for Oen's data. The values of displacement cross section calculated by Alexander are about 20–40% lower than the values calculated in this work. As pointed out before (Alexander, 1997), this difference is likely caused by two factors: the use in Alexander's work of the McKinley–Fesbach approximation, where Oen used the more exact Mott series, and from Oen's use of the unmodified Kinchin–Pease model. The two effects combined increase the total value of the displacement cross-section in the present by about 25% relative to the values calculated by Alexander. It is clear from the calculated gamma displacement cross sections provided in Fig. 4 that atomic displacement due to the Compton scattering is dominant throughout the gamma energy range (up to 14 MeV) for lighter elements ($Z < 0$). For heavier elements, both photoelectric effect at low energy and pair production at high energy become an important source of atomic displacements. The contribution of the photoelectric effect to displacements is relatively weak for lighter elements [Fig. 4(a)]. For heavier elements at lower gamma energy, however, its contribution is dominant, as shown in Fig. 4(b).

As can be seen in Table 1, the increase in E_d from 24 to 40 eV decreases the generation of energetic electrons, which results in the lower atomic displacement cross sections. For example, the calculated total displacement cross sections for iron at $E_d = 24$ eV are 1.8 to 3.9 times higher than those at $E_d = 40$ eV depending on gamma energy.

The effect of secondary displacements on the overall displacement is displayed in Fig. 6. It is highly probable that high energy gamma rays would produce energetic electrons. As the gamma energy increases, the probability of creating secondary displacement increases, so that the cascade contribution to damage also increases. This effect is negligible below a gamma energy of 1.5 MeV and represents about a factor of two increase for a gamma energy of 14 MeV.

5. Conclusion

We have performed a simple evaluation of the gamma atomic displacement cross section as a function of energy in the range 0–14 MeV for the three relevant processes of gamma–electron interaction; photoelectric effect, Compton scattering and pair production. The calculations were performed at two values of the displacement energy. We also evaluated the importance of secondary atomic displacements in the gamma displacement process (cascade effect vs. single displacements). The results show that for lighter elements the Compton displacement cross section dominates throughout the energy range, while for heavier elements, the impact of photoelectric effect at lower energies and pair production at higher energies is important.

Acknowledgements

We thank L.R. Greenwood for providing the SPECTER code. This work was supported by the FERMI Utilities Consortium (which includes GPU Nuclear, PSE&G, PP&L, PECO, Commonwealth Edison and Westinghouse).

References

Alexander, D.E., Rehn, L.E., 1994. Gamma-ray displacement damage in the pressure vessel of the advanced boiling water reactor. Journal of Nuclear Materials 217, 213–216.

Alexander, D.E., 1997. Defect production considerations for gamma ray irradiation of reactor pressure vessel steels. Journal of Nuclear Materials 240, 196–204.

Baumann, N.P., 1990. Gamma ray induced displacements in D20 reactors. In: Proceedings of the 7th ASTM EURATOM Symposium on Reactor Dosimetry. Strasbourg, France, 1990. Kluwer, New York, pp. 689–697.

Cember, H., 1983. Introduction to Health Physics. Pergamon Press, New York.

Davisson, C.M., Evans, R.D., 1952. Gamma-ray absorption coefficients. Reviews of Modern Physics 24 (2), 79–95.

Evans, R.D., 1955. The atomic nucleus. McGraw-Hill, New York.

Farrell, K., Mahmood, S.T., Stoller, R.E., Mansur, L.K., 1994. An evaluation of low temperature radiation embrittlement mechanisms in ferritic alloys. Journal of Nuclear Materials 210, 268–281.

Greenwood, L.R., Smither, R.K. 1985. Specter: Neutron Damage Calculations for Materials Irradiations. Argonne National Laboratory.

Oen, O.S., Holmes, D.K., 1959. Cross sections for atomic displacements in solids by gamma rays. Journal of Applied Physics 30 (8), 1289–1295.

Oen, O.S. 1973. Cross sections for atomic displacements in solids by fast electrons. Oak Ridge National Laboratory Report No. ORNL-4897.

Rehn, L.E., Birtcher, R.C., 1993. Experimental studies of free defect generation during irradiation — implications for reactor environments. Journal of Nuclear Materials 205, 31–39.